
Phase I Therapy Study of ^{186}Re -Labeled Chimeric Monoclonal Antibody U36 in Patients with Squamous Cell Carcinoma of the Head and Neck

David R. Colnot, Jasper J. Quak, Jan C. Roos, Arthur van Lingen, Abraham J. Wilhelm, Gerard J. van Kamp, Peter C. Huijgens, Gordon B. Snow, and Guus A.M.S. van Dongen

Departments of Otolaryngology/Head and Neck Surgery, Nuclear Medicine, Clinical Chemistry, and Hematology, University Hospital Vrije Universiteit, Amsterdam, The Netherlands

A phase I therapy study was conducted to determine the safety, maximum tolerated dose (MTD), pharmacokinetics, dosimetry, immunogenicity, and therapeutic potential of ^{186}Re -labeled anti-CD44v6 chimeric monoclonal antibody (cMAb) U36 in patients with squamous cell carcinoma of the head and neck (HNSCC). The potential of a diagnostic study with $^{99\text{m}}\text{Tc}$ -cMAb U36 to predict the biodistribution of ^{186}Re -cMAb U36 was evaluated. **Methods:** Thirteen patients with recurrent or metastatic HNSCC were given 750 MBq $^{99\text{m}}\text{Tc}$ -cMAb U36 (2 mg) followed 1 wk later by a single dose of ^{186}Re -cMAb U36 (12 or 52 mg) in radiation dose-escalating steps of 0.4, 1.0, and 1.5 GBq/m². After each administration, planar and SPECT images were obtained, and the pharmacokinetics and development of human antimurine as well as anti-cMAb responses were determined. Radiation absorbed doses to tumor, red marrow, and organs were calculated. **Results:** Administration was well tolerated, and excellent targeting of tumor lesions was seen in all patients. Dose-limiting myelotoxicity (thrombocytopenia being most prominent) was the only toxicity observed, resulting in grade 4 myelotoxicity in 2 patients treated with 1.5 GBq/m². The MTD was established at 1.0 GBq/m², at which a transient grade 3 thrombocytopenia was seen in 1 patient. One patient showed stable disease for 6 mo after treatment at the MTD. The 2 patients with dose-limiting myelotoxicity showed a marked reduction in tumor size. The reduction was of short duration and, therefore, not considered an objective response. Tumor absorbed doses at MTD ranged from 3.0 to 18.1 Gy. Red marrow doses ranged from 20 to 112 cGy (mean, 51 ± 16 cGy/GBq) and correlated with platelet nadir ($r = 0.8$; $P < 0.01$). Pharmacokinetics varied between patients treated at the same dose level and were accurately predicted by the diagnostic procedure. Five patients experienced a human anti-cMAb response, 1 of which was a human antimouse antibody response. **Conclusion:** This study shows that ^{186}Re -cMAb U36 can be safely administered, with dose-limiting myelotoxicity at 41 mCi/m². The use of cMAb U36 instead of its murine counterpart did not decrease the induction of human antibody responses. The availability of a $^{99\text{m}}\text{Tc}$ -labeled diagnostic study that can predict the pharmacokinetics of ^{186}Re -cMAb U36 offers the possibility of using such a study for selection of a safe radioimmunotherapy dose.

Key Words: radioimmunotherapy; monoclonal antibodies; ^{186}Re ; dosimetry; pharmacokinetics; head and neck cancer

J Nucl Med 2000; 41:1999–2010

Squamous cell carcinoma of the head and neck (HNSCC) accounts for approximately 5% of all newly diagnosed malignancies in northwestern Europe and the United States, and the worldwide incidence is 500,000 cases each year (1). Despite improvements in locoregional treatment by surgery and radiotherapy for stages III and IV (70%), the failure rate, either locally or at distant sites, is still high. An effective adjuvant systemic treatment is therefore needed to improve survival in this patient group.

Among the novel approaches for selective treatment is the use of monoclonal antibodies (MAbs) conjugated with radionuclides. In the last decade, successful treatment with radioimmunotherapy (RIT) of hematologic malignancies refractory to chemotherapy has been reported (2,3). However, for solid tumors such results have not yet been reached, although some studies have reported encouraging results with RIT for small metastatic lesions or as adjuvant treatment (4–8). To date, most clinical RIT studies have been performed with ^{131}I . However, the low percentage (33%) of therapeutic β -emission of ^{131}I is suboptimal, and its abundant γ -emission can cause an unnecessary radiation burden for medical personnel and relatives, requiring extensive radiation safety measures. ^{186}Re is considered to be a better candidate, because almost all decay (91%) is by therapeutic β -emission with an ideal energy for eradicating minimal residual disease: a maximum β -energy of 1.07 MeV, and 90% of it delivered within 1.8 mm of a point source (9,10). The 9% γ -emission has excellent imaging properties for scintigraphy and dosimetry and results in minimal radiation exposure of medical personnel. Its physical half-life of 3.7 d is considered compatible with the time needed for intact MAbs to achieve optimal tumor-to-nontumor ratios. To date, few studies have been performed with ^{186}Re -labeled MAbs (11–13).

Received Dec. 14, 1999; revision accepted May 5, 2000.

For correspondence or reprints contact: Guus A.M.S. van Dongen, PhD, Department of Otolaryngology/Head and Neck Surgery, University Hospital Vrije Universiteit, De Boelelaan 1117, P.O. Box 7057, 1007 MB Amsterdam, The Netherlands.

Murine MAb (mMAb) U36 has been extensively studied in patients with primary HNSCC and lymph node metastases undergoing surgery (14,15). Tumor uptake values up to 43% of the injected dose per kilogram (%ID/kg) of tumor were reached, with a mean value of 20.4 %ID/kg 2 d after administration (14). Immunohistochemistry has shown reactivity with 99% of primary HNSCC and a homogeneous reactivity pattern with 96% of these tumors, making the antibody an ideal candidate for targeting nearly all HNSCC (16). The antigen recognized by MAb U36 is the v6 domain of the CD44 glycoprotein (17). The development of human antimouse (HAMA) responses in patients treated with mMAb U36 could hamper its use for multiple-treatment RIT, and a chimeric MAb (cMAb) U36 was therefore constructed.

This phase I radiation dose-escalation trial with ^{186}Re -labeled cMAb U36 was performed on HNSCC patients to determine safety, dose-limiting toxicity, and maximum tolerated dose (MTD). The pharmacokinetics, biodistribution, immunogenicity, imaging, dosimetry, and therapeutic effects were studied to evaluate its potential for adjuvant treatment of HNSCC. The feasibility of a scouting study with $^{99\text{m}}\text{Tc}$ -labeled cMAb U36, given 1 wk before RIT to predict the biodistribution of cMAb U36, was assessed.

MATERIALS AND METHODS

Patient Eligibility

Patients with clinical evidence of recurrent HNSCC, either locally or at distant sites, refractory to conventional therapy or for whom no curative options were available were candidates. A histologically confirmed HNSCC in the past was required for inclusion. Other eligibility criteria were an age between 18 and 80 y, a Karnofsky performance status of at least 60, and a life expectancy of at least 3 mo. An interval of at least 6 wk from the last chemotherapy or radiotherapy was required, as well as good recovery after prior treatment. Patients were excluded if their white blood cell count was less than 3500/ μL , if platelets were less than 150,000/ μL , if the serum creatinine concentration was greater than 150 $\mu\text{mol}/\text{mL}$, or if the bilirubin level was greater than 40 $\mu\text{mol}/\text{mL}$. Other exclusion criteria were pregnancy, past administration of mMAbs, evidence of a life-threatening infection, allergic diathesis, or serious cardiac disease. The study was approved by the Institutional Review Board of the University Hospital Vrije Universiteit, Amsterdam, The Netherlands. All patients gave signed informed consent after receiving a thorough explanation of the study.

cMAb U36

MAb U36 (Centacor B.V., Leiden, The Netherlands) was generated by immunizing BALB/c mice with viable cells of the HNSCC cell line UM-SCC-22B (18). The antigen recognized by MAb U36 is a 200-kDa glycoprotein located on the outer cell surface. Characterization of the target antigen by complementary DNA cloning and sequence analysis revealed that the antigen is identical to keratinocyte-specific CD44 splice variant epican (17). Through screening of overlapping synthetic peptides, the epitope appeared to be located in the v6 domain of CD44 (17). Expression of the v6-containing CD44 variants has been observed for a variety of carcinomas, including head and neck, lung, skin, esophagus, and

cervix, but also for adenocarcinomas of the breast, colon, lung, and stomach (19,20). In patients with carcinoma of the breast and colon and with non-Hodgkin's lymphoma, a correlation has been shown between an overexpression of CD44v6 and reduced survival (21–23). The CD44v6 overexpression is thought to confer metastatic potential to tumor cells (24). Screening of normal tissues has revealed expression in skin keratinocytes, breast and prostate myoepithelium, and bronchial epithelium (18,20,25).

In a previous radioimmunoscinigraphy (RIS) study, HAMA responses were observed in 37% of patients (15). Therefore, for reduction of immunogenicity, a cMAb U36 was constructed containing the murine-variable domains attached to the human $\gamma 1$ heavy-chain and human κ light-chain constant regions using recombinant DNA technology, as has been described (26).

Radiolabeling and Quality Controls

All patients received both $^{99\text{m}}\text{Tc}$ -cMAb U36 and ^{186}Re -cMAb U36. The final quality of each batch of radiolabeled cMAb U36 was tested (27). For coupling of $^{99\text{m}}\text{Tc}$ and ^{186}Re to cMAb U36, the same chelate *S*-benzoyl-mercaptoacetyltriglycine (MAG3) was used as described previously (27,28). The radionuclides and chelate were obtained from Mallinckrodt, Inc. (Petten, The Netherlands). The mean specific activity of ^{186}Re at the time of labeling was 13.2 ± 5.6 MBq/nmol. In short, after synthesis of $^{99\text{m}}\text{Tc}$ -MAG3 or ^{186}Re -MAG3, an esterification with tetrafluorophenol was performed. Subsequently, the ester was purified and conjugated to cMAb U36. Radiolabeled cMAb U36 was purified on a PD10 column (Pharmacia-Biotech, Woerden, The Netherlands) with 0.9% NaCl as eluent for the $^{99\text{m}}\text{Tc}$ -cMAb U36 conjugates and 0.9% NaCl with 5 mg/mL ascorbic acid (pH 5) for the ^{186}Re -cMAb U36 conjugates. Finally, the conjugates were filter sterilized. The ratio of ^{186}Re -MAG3 to cMAb U36 was always lower than 4. The radiochemical purity of the conjugates was more than 93% (mean, 97%), as assessed by high-performance liquid chromatography (HPLC) and thin-layer chromatography of the final product. Each radiolabeled cMAb U36 preparation was assayed for immunoreactivity by measuring binding to 0.1% paraformaldehyde-fixed cells of the HNSCC cell line UM-SCC-11B as described previously (27). The immunoreactive fraction of both $^{99\text{m}}\text{Tc}$ - and ^{186}Re -cMAb U36, as determined by a modified Lineweaver Burk plot, ranged from 77% to 100% (mean, 96%) for all preparations.

Prestudy Screening and Radiologic Assessment

The patients' history and physical condition were examined, and routine laboratory analyses were performed, including serum electrolytes, hepatic enzymes, thyroid and renal function, and urine. Complete blood cell and platelet counts, an electrocardiogram, and a chest radiograph were obtained. CT or MRI scans were obtained as previously described (15).

Tumor volume was assessed by an experienced radiologist drawing regions of interest (ROIs) on consecutive CT or MRI slices with a VoxelQ system (Picker International, Highland Heights, OH), which enables 3-dimensional reconstruction and automated volume calculation. The volume of recurrent tumors or metastases was determined in cubic centimeters and used for tumor dosimetry and evaluation of RIT efficacy. Because of the use of a gantry tilt in some of the CT studies, 3-dimensional reconstruction and automatic volume calculation was not always possible. In these cases, the sum of individual ROI surfaces and slice thicknesses was used for tumor volume estimation and corrected for the degree of gantry tilt.

Study Design

All patients underwent a scouting study before RIT with 2 mg ^{99m}Tc -labeled cMab U36 (750 MBq) to evaluate whether such a procedure could predict the biodistribution of cMab U36. A complete pretreatment assessment was performed before this study, and blood samples were taken for pharmacokinetic analyses. Irrespective of the outcome of the RIS study, RIT was given within 1 wk in escalating dose steps of ^{186}Re -labeled cMab U36. Two patients (patients 1 and 2) received 12 mg cMab U36 labeled with 0.4 GBq/m² ^{186}Re . All other patients received 52 mg cMab U36 labeled with escalating radiation doses. The dose levels were 0.4, 1.0, and 1.5 GBq/m² and were planned to rise with escalating steps of 0.5 GBq/m². Vital functions (blood pressure, pulse rate, breathing rate, and temperature) were assessed before administration; after 20, 40, 60, 120, and 240 min; and at 21 h.

Safety

Patients were admitted for 21 h in a special treatment room at the Department of Nuclear Medicine. Thereafter, they stayed for an additional 3 d in a single room. Dose rates (in $\mu\text{Sv/h}$) were measured directly after administration, and after 21 and 72 h, at distances of 50 and 100 cm with a γ -radiation dose rate counter (Berthold LB 123; EG&G, Ortec, Oak Ridge, TN). The patients were discharged 4 d after administration of ^{186}Re -cMab U36, and the set of pretreatment laboratory analyses was repeated weekly for at least 6 wk. The severity of toxicities was graded according to the National Cancer Institute Common Toxicity Criteria. The MTD was defined as the dose level at which a grade 4 hematologic or grade 3 nonhematologic toxicity developed in not more than 1 of 6 patients. A complete response was defined as disappearance of all measurable disease by physical examination or radiographic criteria for at least 4 wk. A partial response was defined as a reduction of at least 50% in the sum of the products of the perpendicular diameters of all index lesions for at least 4 wk and no new lesions. Stable disease was defined as a 50% reduction or a 25% or smaller increase in the sum of the perpendicular diameter products and no new lesions. This state had to persist for a minimum of 3 mo. Progression was defined as an unequivocal increase in size (>25%) of any lesion or the appearance of a new lesion.

Imaging Studies

The same acquisitions were made for RIS with ^{99m}Tc -cMab U36 as for RIS with ^{186}Re -cMab U36. In the ^{99m}Tc -RIS procedure, simultaneously acquired planar anterior and posterior whole-body scans were obtained within 1 h after administration of the radioimmunoconjugate and after 21 h. For the ^{186}Re procedure, further scans were obtained after 72 and 144 h and, if feasible, for up to 2 wk. For all scintigraphic studies, a large field-of-view gamma camera (Dual Head Genesys Imaging System; ADAC Laboratories, Milpitas, CA) equipped with low-energy high-resolution parallel-hole collimators and connected to a computer system (Pegasys; ADAC Laboratories) was used. Use of the same collimator for ^{99m}Tc -cMab U36 imaging as for ^{186}Re -cMab U36 imaging was expected to result in good image resolution. The low percentage of high-energy gamma photons of ^{186}Re (0.05% > 600 keV) was not expected to require the use of a medium-energy collimator, as was done in other studies (29,30). Camera quality-control measures were taken at each imaging time. With the aliquot retained from the radioimmunoconjugate preparation for injection, a weighed dilution of the injected patient dose was prepared as standard and measured simultaneously during imaging on all whole-body scans. Lateral, anterior, and posterior planar images

and SPECT images of the region of tumor recurrence, that is, the thorax or the head and neck, were acquired at 21 h for ^{99m}Tc -RIS and at 21, 72, and 144 h for ^{186}Re -RIS. Acquisition parameters for planar and SPECT images were as previously described (14). In short, studies were performed with 360° rotation, 64 steps, and postfiltering with a Hanning filter (cutoff at 1 cycle/cm). Imaging results were interpreted by an experienced examiner, who was unaware of the site of recurrence or the presence of distant metastases.

Pharmacokinetics

Blood samples were taken from the opposite antecubital vein at 5, 10, and 30 min and at 1, 2, 4, 16, and 21 h after injection of ^{99m}Tc -as well as of ^{186}Re -cMab U36. For ^{186}Re -cMab U36, additional samples were taken at 72 and 144 h after injection. Whole-blood and plasma samples were counted in a γ multiwell counter (1470 Wizard; Wallac, Turku, Finland), and radioactivity levels were expressed as %ID/kg. Corrections were made for background activity and decay; the %ID/kg was determined by comparison with an aliquot retained from the conjugate preparation for injection. For ^{186}Re -cMab U36, an area under the time-activity concentration curve (AUC) to infinity was calculated using a curve-fitting program (Multifit, Groningen, The Netherlands) to generate monoexponential or biexponential clearance curves. To compare the pharmacokinetic behavior of both radioimmunoconjugates for each individual patient, AUCs from 0 to 25 h after injection were calculated. The biologic half-life was calculated as $t_{1/2}$, or as $t_{1/2\alpha}$ and $t_{1/2\beta}$ for monoexponential and biexponential clearance, respectively, of the radioimmunoconjugate, depending on its best fit. HPLC was performed on plasma samples to assess the percentages of radiolabeled free cMab U36 (retention time, 15.9 ± 0.2 min) and complexed cMab U36 (retention time, 11.1 ± 1.1 min), essentially as described previously (27).

Dosimetry

A biologic whole-body half-life was calculated using least squares fitting of the curve for whole-body time versus %ID. Extrapolation was done from the latest time points to infinity. The conjugate view counting technique was used for quantification of activity in the organs, and the initial whole-body counts were regarded as representing 100% of the injected dose. On all whole-body scans, ROIs were drawn around the following organs: liver, lungs, spleen, and left kidney. For dosimetry of the lungs, a smaller ROI was drawn in the right lung to reduce the contribution of scatter originating from the cardiac blood pool and liver. Total lung counts were obtained by correction of the counts per pixel of the smaller ROI for the total lung size. A background ROI was drawn in the lower left quadrant of the abdomen, and 75% and 50% of the counts were used for background correction of activity in the spleen and kidney, respectively (31). For lung and liver, no background correction was performed. An effective attenuation factor was derived from phantom studies by Breitz et al., (29) who obtained fractions of counts transmitted to examine the attenuation for ^{186}Re . The background subtracted counts from each organ were multiplied by this attenuation factor. Correction for counting efficiency of the gamma camera was done using an imaged standard with ^{186}Re . The %ID was calculated for each organ at each imaging time, and the effective AUC for the whole body as well as for all organs was used to obtain residence times in a spreadsheet software program (Lotus 1-2-3, release 5; Lotus Development Corporation, Cambridge, MA). Residence times were implemented in MIRDOSE3 software (Oak Ridge Associated Universities, Oak

Ridge, TN), to obtain S values and the total absorbed radiation dose per injected dose (cGy/GBq) to organs and the whole body.

Using the whole-blood time–activity concentration curve for ^{186}Re -cMab U36, AUCs to infinity were calculated for red marrow dosimetry. Patient-specific red marrow dosimetry was performed according to the method of Shen et al. (32). This method also considers the contribution of other organs and the whole body. The concentration of intact MAbs in bone marrow is regarded to be 0.2–0.4 times that in circulating blood, and this red marrow-to-blood ratio was determined using the patients' hematocrit and red marrow extracellular fluid fraction (33). A comparable clearance from blood and red marrow was assumed, as well as a uniform distribution throughout the red marrow.

An ROI for the tumor was drawn on the anterior whole-body scan obtained at 72 h after injection and then copied to anterior scans acquired at other times. Another ROI was drawn for tumor background correction on the contralateral side of the neck. The relative tumor-to-neck diameter, as assessed with CT or MRI, was used for background correction according to the method of Buijs et al. (31). Background-subtracted counts were corrected for attenuation depending on tumor depth derived from CT or MRI results and the effective attenuation factor (29). Tumor volume was measured to obtain S values for tumor nodules using MIRDOSE3 software. The tumor absorbed dose estimates were obtained after implementation of the residence times in MIRDOSE3 software. For each evaluable patient, the ratio of tumor absorbed dose to red marrow absorbed dose was determined.

Human Anti-cMab U36 Response

To evaluate the immunogenicity of cMab U36, a human anti-cMab (anti-isotypic, HACA) assay was performed. To evaluate whether there were responses against the murine part (anti-idiotypic, HAMA), a second assay was included. Human antibody response was tested in patients' sera before administration of $^{99\text{m}}\text{Tc}$ - and ^{186}Re -cMab U36, and 1 and 6 wk after the start of RIT. For the detection of HAMA, an enzyme-linked immunosorbent assay (ELISA) with mMab U36 was used as described previously (15). In short, ELISA plates were coated with goat polyclonal antimouse IgG, followed by mMab U36 solution. Prediluted patient serum samples were added, and for detection, rabbit polyclonal antihuman IgG conjugated with horseradish peroxidase (HRP) followed by *o*-phenylenediamine was used. The sensitivity of the HAMA assay was at a titer of 50. A HAMA titer of 3 times this limit (>150) was arbitrarily considered positive.

The concentration of HACA was measured by coating a microtiter plate (Costar Europe Ltd., Badhoevendorp, The Netherlands) with cMab U36 IgG, 2 μg per well, in phosphate-buffered saline (PBS), pH 7.2, and incubating overnight at room temperature. After the contents were discarded, the plate was blocked with 200 μL assay buffer per well (1% volume in volume newborn calf serum [BioWhittaker, Verviers, Belgium] in PBS with 0.02% Tween 20 [Sigma, Zwijndrecht, The Netherlands]) by incubation at 37°C for 1 h. The wells were then washed with 200 μL wash buffer per well (PBS with 0.05% Tween 20). Thereafter, 100- μL standard dilutions of rabbit antihuman IgG (A0424; Dako, Glostrup, Denmark) in assay buffer and diluted patients' serum (1:10 in assay buffer) were pipetted into the wells and incubated on an orbital shaker at 400 rpm for 1 h at room temperature. The rabbit antihuman IgG was used to construct a calibration curve. The wells were washed, and after the addition of 100 μL biotinylated cMab U36 in assay buffer (1 μg per well), the plate was incubated as in

the previous step. After washing, the wells were incubated with 100 μL (10 ng per well) poly-HRP-conjugated streptavidin (CLB, Amsterdam, The Netherlands) in assay buffer for 20 min at 400 rpm at room temperature. The wells were then washed, and HRP activity was determined by adding 100 μL tetramethylbenzidine substrate solution per well (100 mg/L tetramethylbenzidine in 0.1 mol/L sodium acetate and citric acid buffer [pH 4.0]) and incubating for 30 min in the dark at room temperature. The reaction was stopped with 50 μL 2N H_2SO_4 per well, and the absorption was measured at 450 nm in a microtiter plate reader. The sensitivity of the HACA assay was at a concentration of 0.2 mg/L. The intraassay coefficient of variation (CV), as calculated from duplicate measurements in serum samples with test results greater than the detection limit, was 6.5%. A HACA test value 3 times this limit, or >0.6 mg/L, was arbitrarily considered positive.

Statistical Analysis

All mean values reported represent arithmetic means with corresponding SDs. Associations between variables were calculated with SPSS 7.5 software (SPSS Inc., Chicago, IL) using Pearson correlation tests. Two-sided significance levels were calculated for all parameters, with $P < 0.05$ considered statistically significant.

RESULTS

Thirteen patients (10 men, 3 women; age range, 47–68 y; mean age, 57 y) entered this study. Their characteristics are shown in Table 1.

Safety and Nonhematologic Toxicity

All administrations of $^{99\text{m}}\text{Tc}$ - and ^{186}Re -cMab U36 were well tolerated by the patients, and no signs of acute adverse events were observed. No relevant changes occurred in physical parameters during the first few days after administration, and no changes in blood parameters indicated toxicity of organs such as the liver or kidneys. Although in some patients accumulation of radioactivity in feces was visible by scintigraphy, no symptoms of gastrointestinal radiation toxicity were observed. Two weeks after ^{186}Re -cMab U36 administration, bilateral erysipelas developed in the face of patient 2 and was effectively treated with antibiotics. Patient 5 died 2 d after administration of ^{186}Re -cMab U36, most likely because of cardiopulmonary insufficiency or a myocardial infarction. In this patient, scintigraphy 21 h after administration of $^{99\text{m}}\text{Tc}$ -cMab U36 showed relatively high uptake in the lungs, but this was not observed on images obtained after ^{186}Re -cMab U36 injection. This apparent difference was considered to be related to the difference in MAb doses used in RIS and RIT. No other signs indicating a possible relationship between antibody administration and death were noticed, but the possibility of a relationship could not be excluded.

Mean radiation dose rates 1 m from the patients treated with the highest dose were 3.2 $\mu\text{Sv/h}$ directly after injection and 1.6 $\mu\text{Sv/h}$ at discharge 3 d after injection. These dose rates would result in cumulative doses far less than the annual limit of 2 mSv considered acceptable for medical personnel and family members.

TABLE 1
Patient and Tumor Characteristics

Patient no.	Sex	Age (y)	Site of disease	Prior treatment	
				Radiotherapy	Chemotherapy
1	M	53	Oropharynx	Yes	MTX
2	F	54	Posterior pharyngeal wall	Yes	None
3	M	54	Oropharynx	Yes	None
4	M	47	Oropharynx	No	None
5	M	56	Piriform sinus, left and right parapharyngeal area	Yes	Cis + 5-FU
6	M	66	Larynx and cystic lesion, neck, right side	Yes	Cis + Gem/MTX
7	F	56	Oropharynx, both sides	Yes	None
8	M	58	Hypopharynx	Yes	None
9	M	67	Neck recurrence, left side	Yes	None
10	M	68	Oropharynx, right axilla metastasis	Yes	None
11	M	52	Larynx	Yes	None
12	M	52	Floor of mouth, submental recurrence	Yes	Cis + Gem
13	F	59	Esophagus	Yes	None

MTX = methotrexate; Cis = cisplatin; 5-FU = fluorouracil; Gem = gemcitabine.

Hematologic Toxicity

The red marrow appeared to be the dose-limiting organ. Myelotoxicity consisted mainly of thrombocytopenia, with a nadir 4 wk after RIT. At the lowest dose level—0.4 GBq/m²—no clinically relevant hematologic toxicity was seen, whereas at the next dose level—1.0 GBq/m²—only mild toxicity was observed (Table 2). In 1 patient at this dose level (patient 6), grade 3 thrombocytopenia and grade 1 leukocytopenia developed, and the patient recovered from both conditions within 1 wk. He had been treated 14 mo before RIT with 2 courses of cisplatin and gemcitabine and had received a weekly dose of 60 mg methotrexate for 20 wk 6 mo before RIT. Of 3 patients treated with 1.5 GBq/m²,

grade 4 thrombocytopenia developed in 2. One of these 2 (patient 13), who had never been treated with chemotherapy, recovered within 1 wk from grade 4 thrombocytopenia and grade 2 leukocytopenia. The other patient (patient 12) had previously experienced myelotoxicity as a result of 3 courses of cisplatin and gemcitabine, given 6 mo before entry into the RIT study, but hematologic parameters had recovered to baseline. In that patient, grade 4 thrombocytopenia and leukocytopenia developed 4 wk after administration of ¹⁸⁶Re-cMAb U36, and he died from an opportunistic lung infection shortly thereafter. Autopsy confirmed bilateral bronchopneumonitis with signs of an adult respiratory distress syndrome resulting from pneumonia caused by a

TABLE 2
Absorbed Dose Estimates and Myelotoxicity

Patient no.	Dose (GBq/m ²)	Total administered dose (GBq)	Absorbed dose, whole body (cGy/GBq)	Absorbed dose, red marrow (cGy)	Platelet nadir	Toxicity grade	WBC nadir	Toxicity grade	Granulocyte nadir	Toxicity grade
1	0.4	0.48	35.1	46	230	0	3.4	1	2.3	0
2	0.4	0.59	24.3	25*	NA	NA	NA	NA	NA	NA
3	0.4	0.70	32.4	30	200	0	6.1	0	5.2	0
4	0.4	0.70	35.1	20	285	0	5.7	0	4.1	0
5	1.0	1.60	21.6	73*	NA	NA	NA	NA	NA	NA
6	1.0	2.11	21.6	109	37	3	3.6	1	2.1	0
7	1.0	1.63	NA	91	206	0	5.3	0	4.5	0
8	1.0	1.70	37.8	77	97	1	4.7	0	3.7	0
9	1.0	1.70	29.7	110	190	0	7.6	0	6.2	0
10	1.0	1.78	29.7	100	126	0	4.9	0	3.4	0
11	1.5	2.96	27.0	104	118	0	4.3	0	3.2	0
12	1.5	2.18	8.1	107	24	4	0.6	4	0.1	4
13	1.5	2.15	29.7	112	22	4	2.3	2	1.8	1

*Patients 2 and 5 did not complete follow-up for evaluation of hematologic toxicity and are therefore not included for analysis of correlation between red marrow dose and development of hematologic toxicity.

WBC = white blood cell count; NA = not available.

mixture of *Streptococcus pneumoniae*, *Escherichia coli*, and *Pseudomonas aeruginosa*. Although the red marrow was greatly aplastic, some erythropoietic activity was seen. On the basis of the results, 1.0 GBq/m² was regarded to be the MTD level.

Imaging

Whole-body scans obtained directly after administration of ¹⁸⁶Re-cMAB U36 showed mainly blood-pool activity, which was decreasing over time but clearly present up to 72 h after injection in most patients. Representative whole-body scans are shown in Figure 1. At later intervals, a homogeneous distribution was observed in the lungs, liver, spleen, and kidneys, except for increased uptake at tumor sites. In general, no selective accumulation at nontumor sites was visible, except in feces and urine (bladder). In 1 patient, a relatively high accumulation was seen in the liver at 21 h after injection. This patient (patient 2) also had relatively rapid clearance of ¹⁸⁶Re-cMAB U36 from the blood.

Scintigraphy after administration of ^{99m}Tc- and ¹⁸⁶Re-cMAB U36 showed a similar biodistribution, including comparable uptake at tumor sites in the head and neck (Fig. 2). Planar and SPECT images obtained at later intervals with ¹⁸⁶Re-cMAB U36 showed improved delineation of small lesions and distant metastases. These concerned mainly lung metastases, of which visualization was hampered by the presence of blood-pool activity, requiring imaging at later intervals (Fig. 3). Because of the small size of some lung metastases, not all detected with CT could be detected with planar imaging or SPECT of the chest. Prolonged high blood-pool activity in 1 patient (patient 13) disturbed the visualization of a tumor in the distal esophagus, because the tumor was directly posterior to the heart. A palpable, cytologically proven, 2 × 4 cm metastasis in the right axilla

of patient 10 was not detected by scintigraphy during RIT. High uptake in the lungs was seen in patient 5 on whole-body scans obtained at 21 h after administration of ^{99m}Tc-cMAB U36. Imaging at 21 h after administration of ¹⁸⁶Re-cMAB U36 did not show this high uptake. Patient 7 showed increased uptake in a decubitus lesion on her left shoulder.

Pharmacokinetics

HPLC analysis of the conjugates for injection showed a monomeric peak, with more than 97% of the radioactivity bound to cMAB U36. In plasma samples taken after administration of ¹⁸⁶Re-cMAB U36, HPLC analysis identified monomeric radiolabeled cMAB U36 (retention time, 15.9 ± 0.2 min) and a second small peak corresponding to less than 5% of the total radioactivity, representing complexed cMAB U36 (retention time, 11.1 ± 1.1 min). Therefore, all radioactivity in plasma was assumed to be monomeric radiolabeled cMAB U36, and pharmacokinetic analysis was based on these data. For ¹⁸⁶Re-cMAB U36, in most patients a biexponential whole-blood disappearance could be described with a mean rapid distribution-phase half-life ($t_{1/2\alpha}$) of 7.2 ± 5.1 h, followed by a slower elimination-phase half-life ($t_{1/2\beta}$) of 80.0 ± 36.6 h. Accurate assessment of these parameters for ^{99m}Tc-cMAB U36 was hampered by the limited number of measurements at times later than 21 h after injection. The effective AUCs to infinity to be used for red marrow dosimetry of ¹⁸⁶Re-cMAB U36 ranged from 4.6 to 24.6 GBq × h/L. Biologic AUCs for both ^{99m}Tc- and ¹⁸⁶Re-cMAB U36, as determined up to 25 h after injection, showed variability between patients but, if compared for individual patients, showed a strong correlation ($r = 0.94$; $P < 0.01$), as is illustrated in Figure 4.

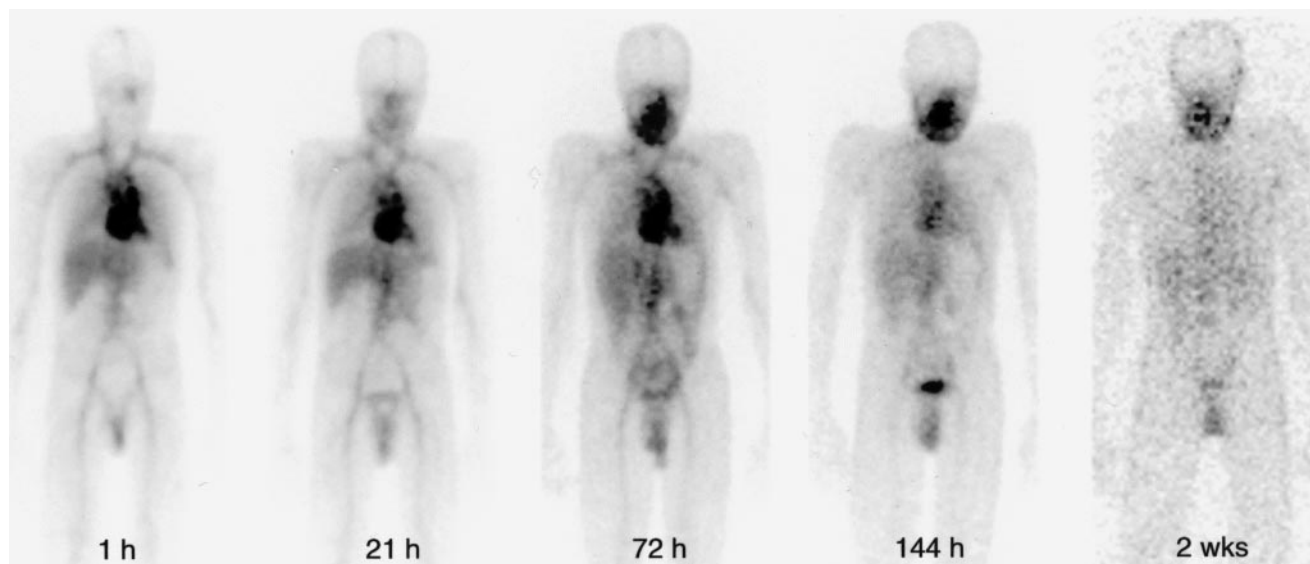


FIGURE 1. Whole-body scans of patient 4 acquired within 1 h after administration of ¹⁸⁶Re-cMAB U36 and after 21, 72, and 144 h and 2 wk. Immediately after injection, most prominent activity is in blood pool. This activity remains high up to 72 h after injection. Relative uptake of radioimmunoconjugate in tumor in right oropharynx increases over time. Tumor becomes better delineated as background activity decreases.

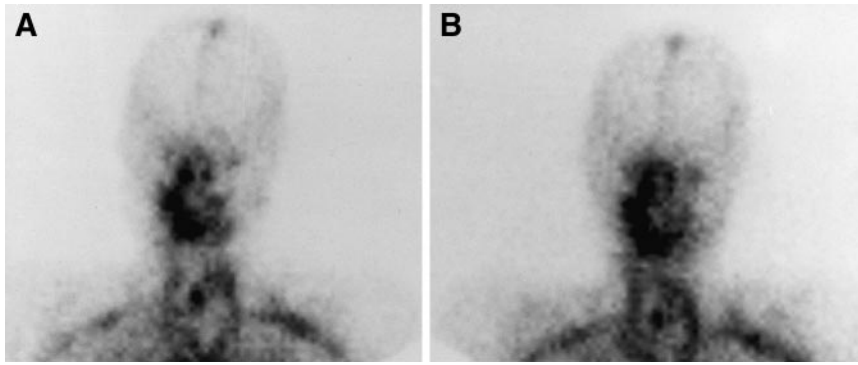


FIGURE 2. Comparison of planar imaging of head and neck region of patient 1 21 h after administration of ^{99m}Tc -cMAB U36 (A) and ^{186}Re -cMAB U36 (B). Accumulation of radiolabeled cMAB U36 is visible at tumor recurrence in right oropharynx.

Human Anti-cMAB U36 Response

HACA and HAMA immune responses were evaluable for all patients except patient 5. Five of the 12 evaluable patients showed a HACA response (Table 3). In 3 of these patients, elevated HACA levels were observed within 1 wk after the ^{99m}Tc -cMAB U36 study procedure, before the start of ^{186}Re -cMAB U36 RIT. One of these patients (patient 6) already showed detectable HACA levels before cMAB U36 administration. He had never before been exposed to mMABs or cMABs. In 3 patients with an immune response, the highest HACA levels were found 1 wk after the start of RIT. One of the patients with a HACA response also showed elevated HAMA titers, indicating that only in this patient had antibodies directed against the murine-variable regions been formed.

Dosimetry

Assuming a homogeneous distribution, absorbed dose to the whole body could be estimated for 12 patients (Table 2). One patient (patient 7) was not able to complete the series of whole-body images, and planar serial regional imaging was done. The whole-body absorbed self-dose was 27.0 ± 5.4 cGy/GBq. The mean biologic whole-body half-life was 344 ± 164 h. For liver, lungs, spleen, and kidneys, calculated absorbed dose estimates to organs were 132.4, 200.0, 137.8, and 135.1 cGy/GBq, respectively.

Red marrow doses, determined from the whole-blood time- ^{186}Re activity concentration curve, ranged from 20 to 112 cGy. The mean radiation dose to the red marrow was 51.4 ± 16.2 cGy/GBq. The most frequently observed myelotoxicity, that is, the decrease in the number of platelets, correlated with the red marrow dose ($r = 0.8$ [$P < 0.01$] for platelet nadir and $r = 0.6$ [$P < 0.05$] for the percentage decrease from baseline platelet counts) (Fig. 5). A significant correlation was found between red marrow dose and decrease in granulocytes ($r = 0.7$ [$P < 0.05$] for the percentage decrease and $r = 0.6$ [$P < 0.05$] for the granulocyte nadir). No significant correlation was found between red marrow dose and decrease in white blood cell count.

Tumor dosimetry was possible for 10 patients (Table 4). The volumes of these lesions ranged from 14 to 135 cm³. The ROI method on whole-body scans revealed the highest tumor uptake values at 72 h after injection, with a mean

uptake of 18.6 ± 9.1 %ID/kg. The mean tumor absorbed dose was 486.5 ± 297.3 cGy/GBq, with tumor doses ranging from 3.0 to 18.1 Gy at the MTD. For the 10 patients evaluable with tumor dosimetry, the ratio between tumor absorbed dose and red marrow absorbed dose was 11.2 ± 8.7 .

Tumor Response

One patient (patient 8), treated at the dose level of 1.0 GBq/m², had stable disease for 6 mo as assessed with CT. At the highest dose level—1.5 GBq/m²—obvious tumor shrinkage was observed in 2 patients. A marked reduction in the size of a tumor in the esophagus (patient 13) was observed 3 wk after administration of ^{186}Re -cMAB U36 (Fig. 6). This tumor partly compressed a stent placed in the esophagus, and after RIT a 60% decrease in tumor size was observed simultaneously with relaxation of the stent. Another patient (patient 11) showed a reduction in the size of a bulky tumor recurrence located submentally and of a lymph node metastasis on the right side of the neck. These two antitumor effects were observed in the 1.5 GBq/m² group and did not meet the criteria for an objective response because of a short duration. In other patients, who experienced disease progression under previous treatment, RIT stabilized the growth of some of the lesions. These stabilizations did not meet the criteria for objective response and included small lung metastases (patients 1 and 7) that seemed unchanged while other neck lesions progressed.

DISCUSSION

RIT with ^{186}Re -cMAB U36 seems to be safe, and no side-effects were observed in this phase I study besides dose-limiting myelosuppression at the ^{186}Re dose level of 1.5 GBq/m². The MTD of 1.0 GBq/m² as found for ^{186}Re -cMAB U36 is considerably lower than has been described for other ^{186}Re -labeled MABs in dose-finding studies. For mMAB NR-LU-10, the MTD was established at 3.3 GBq/m², whereas for cMAB NR-LU-13, the MTD was found to be 2.2 GBq/m² (11,13). This difference can be explained by the longer circulating half-life in blood of cMAB U36, compared with the other 2 radioimmunoconjugates. The mean $t_{1/2\beta}$ of cMAB U36 was 80.0 h, whereas for NR-LU-10 and NR-LU-13, a mean $t_{1/2\beta}$ of 26.5 and 36.5 h, respectively, was found. MAB U36 does not bind to the

cellular fraction of the bone marrow, and no patients with bone metastases participated in this study, nor did RIS reveal increased radioactivity uptake in the red marrow.

Myelotoxicity consisted mainly of thrombocytopenia, with a nadir 4 wk after administration of ^{186}Re -cMab U36. Grade 4 thrombocytopenia was observed at the highest dose level— 1.5 GBq/m^2 —for 2 patients, whereas grade 3 thrombocytopenia developed in 1 of 5 evaluable patients at the MTD level. Leukocytopenia of a grade higher than 3 was seen only at the 1.5 GBq/m^2 dose level. The development of

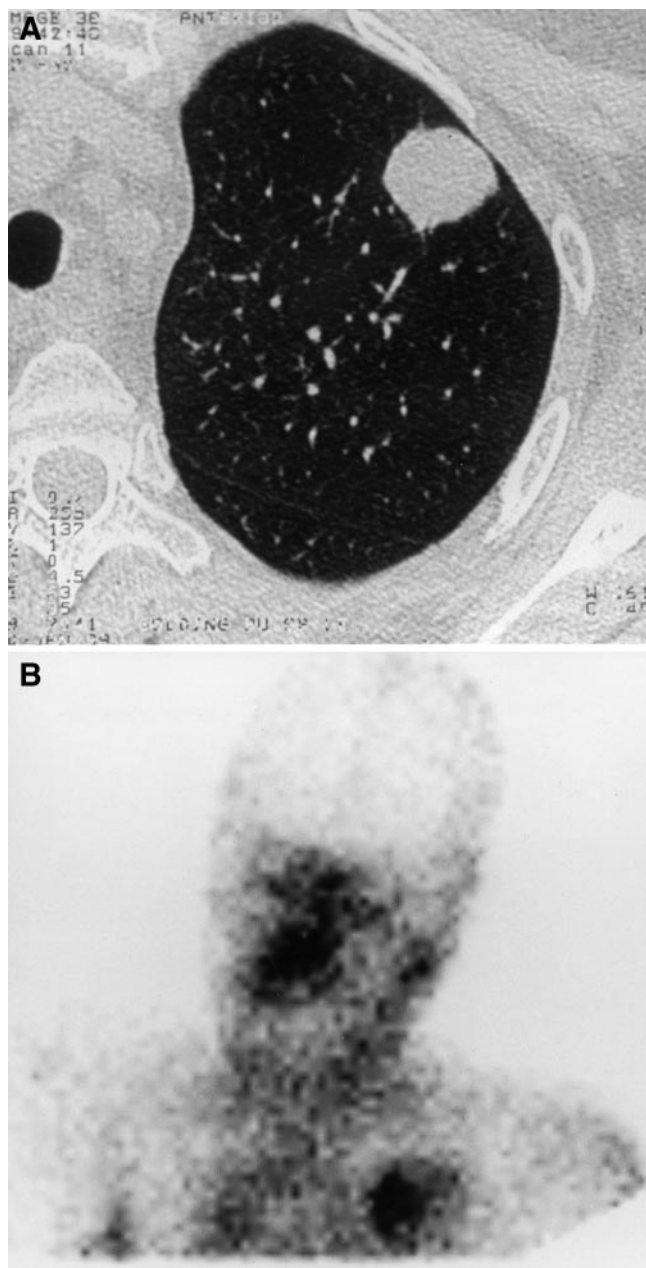


FIGURE 3. CT scan (A) and planar anterior gamma camera scan (B) of patient 7 obtained 144 h after administration of ^{186}Re -cMab U36 show targeting of lung metastasis in upper lobe of left lung. Accumulation of ^{186}Re -cMab U36 is also visible on both sides of oropharynx, where recurrent tumor is present.

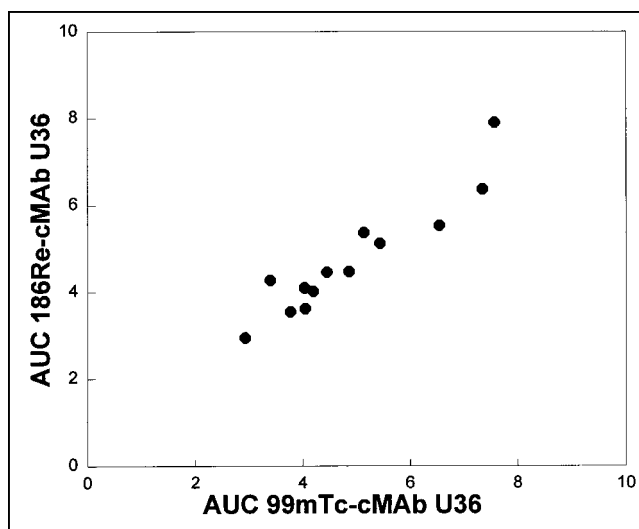


FIGURE 4. Relationship between AUC (expressed as $\%ID \times h$) determined for 0–25 h after injection for individual patients, both for $^{99\text{m}}\text{Tc}$ -cMab U36 (horizontal axis) and for ^{186}Re -cMab U36 (vertical axis). Although relatively large variations are seen between patients, pharmacokinetic behavior of the 2 conjugates seems similar for individual patients ($r = 0.94$; $P < 0.01$).

thrombocytopenia could be related to the red marrow dose, calculated from the whole-blood time- ^{186}Re activity curve.

Because cMab U36 clearance differed considerably between patients in the same dose group and resulted in thrombocytopenia of variable severity, an individualized radiation dose selection for cMab U36 RIT candidates seemed mandatory. In this study, we evaluated the possibility of using $^{99\text{m}}\text{Tc}$ -cMab U36 for prediction of the ^{186}Re -cMab U36 biodistribution. To limit antigen occupation in the tumor because of such scouting studies, $^{99\text{m}}\text{Tc}$ -cMab U36 was administered at a much lower antibody dose than ^{186}Re -cMab U36: 2 mg versus 52 mg. The overall biodistribution of the conjugates observed with RIS seemed to be the same at 21 h after injection, and comparable targeting of tumor lesions was seen (Fig. 2). At later times, imaging with $^{99\text{m}}\text{Tc}$ -cMab U36 is not feasible because of the short half-life of $^{99\text{m}}\text{Tc}$, which is consistent with the findings of Breitz et al., who evaluated the use of $^{99\text{m}}\text{Tc}$ -labeled NR-CO-O₂ (Fab')₂ to predict ^{186}Re dosimetry (29). Therefore, some distant metastases clearly delineated by ^{186}Re -cMab U36 RIS at later times could not be visualized reliably by $^{99\text{m}}\text{Tc}$ -cMab U36 RIS. Despite the difference in antibody dose, the pharmacokinetic behavior of the $^{99\text{m}}\text{Tc}$ - and ^{186}Re -conjugates appeared to be similar during the first 25 h after injection. The physical half-life compared with the biologic half-life of $^{99\text{m}}\text{Tc}$ -cMab U36, however, did not allow accurate prediction at later times. On the basis of these data, we think that prediction of radiation dose delivery to bone marrow, tumor, and normal tissues in individual ^{186}Re -cMab U36 RIT candidates may be feasible but that because of the short physical half-life of $^{99\text{m}}\text{Tc}$, it is not the ideal radionuclide for such a scouting procedure. A better candidate may be ^{186}Re itself. Data on radiation dose rates

TABLE 3
Human Anti-cMAb U36 Antibody Response

Patient no.	cMAb U36 dose (mg)	Before RIS		Before RIT		1 wk after RIT		6 wk after RIT	
		HAMA titer	HACA (mg/L)	HAMA titer	HACA (mg/L)	HAMA titer	HACA (mg/L)	HAMA titer	HACA (mg/L)
1	2 + 12	<50	<0.2	<50	1.50*	<50	2.05*	<50	0.33
2	2 + 12	<50	<0.2	<50	1.30*	113	5.73*	ND	ND
3	2 + 52	<50	<0.2	<50	<0.2	52	<0.2	55	<0.2
4	2 + 52	ND	ND	<50	<0.2	<50	<0.2	110	<0.2
5	2 + 52	<50	<0.2	<50	<0.2	ND	ND	ND	ND
6	2 + 52	<50	0.7*	<50	1.21*	87	5.29*	133	2.46*
7	2 + 52	<50	<0.2	<50	<0.2	<50	<0.2	510*	1.76*
8	2 + 52	<50	<0.2	<50	<0.2	<50	<0.2	<50	<0.2
9	2 + 52	<50	<0.2	67	<0.2	<50	<0.2	119	<0.2
10	2 + 52	<50	<0.2	<50	<0.2	<50	<0.2	<50	<0.2
11	2 + 52	<50	<0.2	<50	<0.2	<50	<0.2	147	<0.2
12	2 + 52	<50	<0.2	<50	<0.2	136	1.88*	94	1.32*
13	2 + 52	<50	<0.2	<50	<0.2	<50	<0.2	<50	<0.2

*Positive responses.

ND = not done.

HAMA titers and HACA levels were measured before administration of 2 mg ^{99m}Tc-cMAb U36 for RIS and within 1 wk when patients received 12 or 52 mg ¹⁸⁶Re-cMAb U36 for RIT. After start of RIT, HAMA and HACA responses were measured at 1 and 6 wk.

and red marrow dosimetry from this study indicate that up to 370 MBq ¹⁸⁶Re can be safely used as a trace-labeled dose, thus allowing imaging and sampling for pharmacokinetics until 7 d after injection. An advantage of using ¹⁸⁶Re is that just 1 radioimmunoconjugate has to be developed for both the scouting procedure and RIT.

Besides the level of radiation dose delivery to the red marrow, other factors may affect the severity of thrombocytopenia on RIT. For example, among the 3 patients in the 1.5 GBq/m² group, patient 11 received a red marrow dose similar to that received by patient 12 but showed more severe myelotoxicity (grade 4 thrombocytopenia and granu-

locytopenia). This result was most likely related to past myelotoxic treatment. In addition, patient 13 suffered from severe myelotoxicity that could be explained neither by a history of myelosuppressive therapy nor by an increased MAb retention. This result indicated that although scouting procedures are used for individual red marrow dosimetry, individual variation in the development of myelotoxicity can be considerable.

Previous immunohistochemical studies (17–19) revealed that high CD44v6 expression in HNSCC tumors is similar to that in normal squamous epithelia; therefore, we anticipated that acute local toxicity might become apparent in the oral mucosa. However, despite the fact that most patients previously experienced mucositis after external beam irradiation, none of the patients experienced such toxicity during this RIT study, possibly because the target antigen is less accessible in normal mucosa than in HNSCC. Previous biodistribution studies in which tissue uptake of radiolabeled mMAb U36 was assessed by biopsy of the surgical specimen revealed a 2.3 times lower uptake of the MAb in normal mucosa than in HNSCC tissue, at 2 and 7 d after injection (14,15). Moreover, for dosimetric calculations one must consider that a part of the disintegration energy dissipates outside the distribution volume of the tissue. Maraveyas et al. (34) reconstructed a larynx phantom and concluded that, for ¹⁸⁶Re, the absorbed fraction in normal mucosal linings will be about 1.6 times less than in HNSCC tissue, leading to a greater tumor-versus-mucosa dose advantage.

In previous RIS studies with ^{99m}Tc-labeled mMAb U36, HAMA responses were observed in 5 of 9 patients (56%) when using the same criteria for positivity as in this study (15). With the aim of reducing immunogenicity, cMAb U36

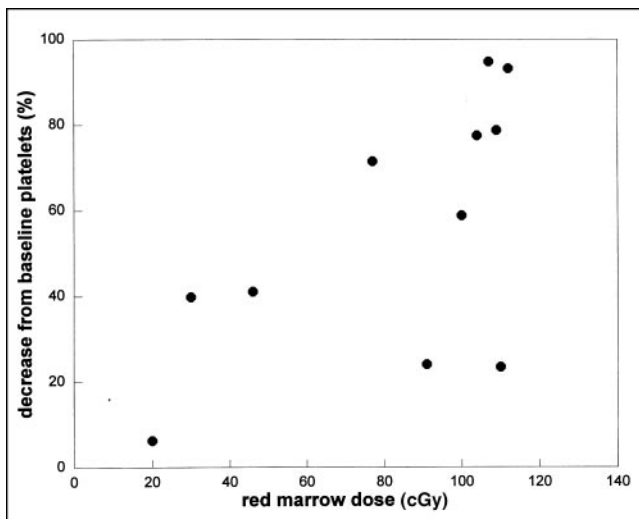


FIGURE 5. Relationship between red marrow dose derived from whole-blood time–activity curve for ¹⁸⁶Re-cMAb U36 and percentage decrease from baseline platelet count ($r = 0.6$; $P < 0.05$).

TABLE 4
Tumor Absorbed Dose Estimates and Response

Patient no.	Total administered dose (GBq)	Tumor volume (cm ³)	Total tumor absorbed dose* (Gy)	Tumor absorbed dose (cGy/GBq)	Response	Follow-up (mo)
1	0.48	34	2.0	424.3	Stable lung metastases	4
2	0.59	80	1.8	308.1	Progression	1
3	0.70	37	4.1	578.4	Progression	4
4	0.70	81	6.7	957.1	Progression	3
5	1.60	40	3.0	186.5	NA	NA
6	2.11	ND	ND	ND	Progression	5
7	1.63	32	ND	ND	Stable lung metastases	3
8	1.70	28	3.5	205.4	Stable disease for 6 mo	8
9	1.70	14	18.1	1064.9	Progression	4
10	1.78	74	4.5	248.6	Progression	3
11	2.96	80	16.7	262.2	Progression	6
12	2.18	135	8.3	383.8	Reduction of tumor mass	1
13	2.15	98	ND	ND	Reduction of tumor mass	2

*Ten patients were evaluable for tumor dosimetry. Site of origin of tumors is indicated in Table 1. Only volumes of visualized tumor lesions are included; dosimetry of lung metastases was not possible.

NA = not available; ND = not done.

was constructed. We found HACA responses directed against cMAb U36 in 5 of 12 evaluable patients (42%), and in 1 of these patients (8%) antibodies directed against the murine variable region were found. Although a reduction in the development of HAMA has been achieved (from 56% to 8%) with cMAb U36, our data indicate that in 4 (maybe 5) of these patients antibodies directed against epitopes residing in the human portion or in the murine-human fusion region of the cMAb had developed.

Three patients already showed HACA before the start of RIT. In 2 of these patients, HACA responses were induced by administration of 2 mg ^{99m}Tc-cMAb U36 1 wk before the start of RIT, whereas in the third patient an elevated preimmune HACA level was found. In 1 of these patients (patient 2), a relatively rapid whole-body and blood clearance of ¹⁸⁶Re-cMAb U36 was observed, whereas RIS revealed relatively high accumulation of activity in the liver. This patient had the highest HACA level measured in the study, 5.73 mg/L. The HACA response may be responsible for the rapid blood clearance and liver accumulation of ¹⁸⁶Re-cMAb U36 in this patient. The fact that a rapid blood clearance was not observed for the other 2 patients with increased HACA levels at the start of RIT might have been caused by the lower HACA levels of these patients or the higher cMAb U36 dose (52 mg instead of 12 mg) they received for RIT.

We have not analyzed the patients' sera for human antibodies directed against the MAG3 chelate. However, one can conclude already, at this stage, that immunogenicity of cMAb U36 cannot be neglected when starting new studies with cMAb U36. This conclusion may be particularly true when considering scouting studies or repeated dosing.

The observation of antitumor effects in patients with bulky disease offers opportunities for further development

of RIT as an adjuvant treatment. Tumor uptake, as assessed by ROIs on scintigraphy, agreed with uptake values obtained previously with mMAb U36 (14,15). The calculated tumor absorbed doses ranged from 3.0 to 18.1 Gy for the 1.06 GBq/m² dose group, whereas the mean absorbed dose to the tumor was 486.5 cGy/GBq for all evaluable patients. As shown in Table 4, these tumor doses appear sufficient for antitumor effects. That antitumor effects are caused by immune modulating effects is unlikely, because cMAb U36 was shown to lack antibody-dependent cell-mediated cytotoxicity or complement-dependent cytotoxicity—mediating activity in vitro (15). RIT studies with ¹⁸⁶Re-labeled mMAb E48 in HNSCC-bearing nude mice revealed that with an accumulated dose in the range of 11–34 Gy, complete remissions of 18%–50% could be achieved (35). Breitz et al. (11) found a partial response lasting 7 mo on treatment of a colon cancer patient with 2 cycles of ¹⁸⁶Re-labeled NR-LU-10. The tumor doses were 21 and 7 Gy for the 2 cycles. These data indicate that RIT with ¹⁸⁶Re-cMAb U36 in its current form occasionally can cause antitumor effects. However, for complete tumor eradication the radiation delivery to the lesions should be increased several times, as when applying RIT in an adjuvant setting for treatment of minimal residual disease. Recently, we reported on the relationship between HNSCC size and MAb accumulation (36). Data for this report were obtained from several RIS and biodistribution studies with the anti-HNSCC MAbs E48 and U36 in HNSCC patients. MAb uptake in small-volume tumors (1 cm³) was found to be approximately 4 times higher than uptake in large-volume tumors (>50 cm³). No data are available for MAb uptake in tumor deposits smaller than 1 cm³, but we nevertheless think that the data presented in this article justify the evaluation of RIT with ¹⁸⁶Re-cMAb U36 in an adjuvant setting.

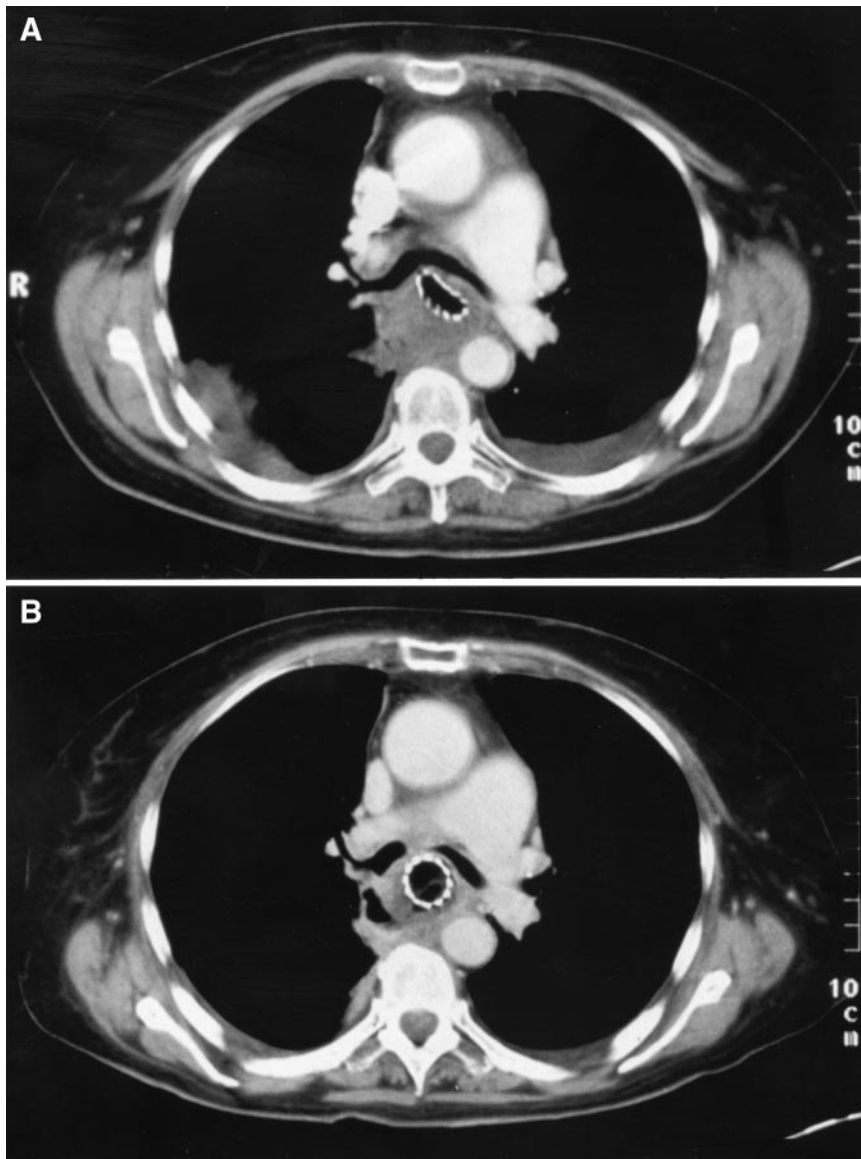


FIGURE 6. (A) CT scan of patient 13 shows large tumor originating from esophagus compressing stent that was placed for palliation 12 mo before RIT. (B) CT scan of same patient 3 wk after administration of 2.15 GBq ^{186}Re -labeled cMAB U36. Sixty percent decrease in tumor size was observed as well as relaxation of stent.

Several other strategies are followed at our institute to improve the efficacy of RIT. Most appealing may be strategies with higher doses of ^{186}Re -cMAB U36 combined with peripheral stem cell reinfusion or a combination of RIT with inhibitors of the epidermal growth factor receptor. In the latter approach, RIT is combined with MAbs or chemical inhibitors capable of blocking epidermal growth factor receptor. In a recent study, we showed that the antiepidermal growth factor receptor MAb 425 strongly enhanced the efficacy of RIT with ^{186}Re -cMAB U36 in HNSCC-bearing nude mice (37). Taking into account the high expression of epidermal growth factor receptor in most HNSCCs and its absence on bone marrow cells, this approach holds promise for future clinical application.

CONCLUSION

RIT with ^{186}Re -cMAB U36 seems safe. The pharmacokinetics of ^{186}Re -cMAB U36 can be predicted by $^{99\text{m}}\text{Tc}$ -cMAB

U36, thus creating the possibility of using such a procedure for selection of a safe RIT dose. However, such a scouting procedure may induce a HACA response. This study shows that tumoricidal doses of ^{186}Re -cMAB U36 can be reached in HNSCC patients with bulky disease. Avenues for RIT are thus opened, especially in an adjuvant setting.

ACKNOWLEDGMENTS

The authors thank Miranda Siegmund for radiolabeling support; Dr. Jonas A. Castelijns for evaluation for CT and MRI examinations; Dr. Wil C.A.M. Buijs for dosimetry discussions; Henri N.J.M. Greuter and Dr. Wim den Hollander for pharmacokinetic determinations; Harry A.M. Twaalfhoven for HAMA and HACA analyses; Peter H. Dignum for supervision on radiation safety issues; and Drs. Remco de Bree, Rik Pijpers, and Emile F.I. Comans for clinical support. This study was supported by the Dutch

REFERENCES

1. Vokes EE, Weichselbaum RR, Lippman SM, Hong WK. Head and neck cancer. *N Engl J Med*. 1993;328:184–193.
2. Kaminski MS, Zasadny KR, Francis IR, et al. Iodine-131-anti-B1 radioimmunotherapy for B-cell lymphoma. *J Clin Oncol*. 1996;14:1974–1981.
3. Liu SY, Eary JF, Petersdorf SH, et al. Follow-up of relapsed B-cell lymphoma patients treated with iodine-131-labeled anti-CD20 antibody and autologous stem-cell rescue. *J Clin Oncol*. 1998;16:3270–3278.
4. Divgi CR, Bander NH, Scott AM, et al. Phase I/II radioimmunotherapy trial with iodine-131-labeled monoclonal antibody G250 in metastatic renal cell carcinoma. *Clin Cancer Res*. 1998;4:2729–2739.
5. Steffens MG, Boerman OC, De Mulder PHM, et al. Phase I radioimmunotherapy of metastatic renal cell carcinoma with 131-I-labeled chimeric monoclonal antibody G250. *Clin Cancer Res*. 1999;5:3268S–3274S.
6. Juweid M, Sharkey RM, Behr TM, et al. Radioimmunotherapy of patients with small-volume tumors using iodine-131-labeled anti-CEA monoclonal antibody NP-4 F(ab')₂. *J Nucl Med*. 1996;37:1504–1510.
7. Behr TM, Sharkey RM, Juweid M, et al. Phase I/II clinical radioimmunotherapy with an iodine-131-labeled anti-carcinoembryonic antigen murine monoclonal antibody IgG. *J Nucl Med*. 1997;38:858–870.
8. Hird V, Maraveyas A, Snook D, et al. Adjuvant therapy of ovarian cancer with radioactive monoclonal antibody. *Br J Cancer*. 1993;68:403–406.
9. Simpkin D, Mackie TT. EGS4 Monte Carlo determination of the beta dose kernel in water. *Med Phys*. 1990;17:179–180.
10. Wessels BW, Rogus RD. Radionuclide selection and model absorbed dose calculations for radiolabeled tumor associated antibodies. *Med Phys*. 1984;11:638–645.
11. Breitz HB, Weiden PL, Vanderheyden J-L, et al. Clinical experience with rhenium-186-labeled monoclonal antibodies for radioimmunotherapy: results of phase I trials. *J Nucl Med*. 1992;33:1099–1109.
12. Jacobs AJ, Fer M, Su FM, et al. A phase I trial of a rhenium 186-labeled monoclonal antibody administered intraperitoneally in ovarian carcinoma: toxicity and clinical response. *Obstet Gynecol*. 1993;82:586–593.
13. Weiden PL, Breitz HB, Seiler CA, et al. Rhenium-186-labeled chimeric antibody NR-LU-13: pharmacokinetics, biodistribution and immunogenicity relative to murine analog NR-LU-10. *J Nucl Med*. 1993;34:2111–2119.
14. De Bree R, Roos JC, Quak JJ, et al. Radioimmunoscintigraphy and biodistribution of ^{99m}Tc-labeled monoclonal antibody U36 in patients with head and neck cancer. *Clin Cancer Res*. 1995;1:591–598.
15. De Bree R, Roos JC, Plaizier MA, et al. Selection of monoclonal antibody E48 IgG or U36 IgG for adjuvant radioimmunotherapy in head and neck cancer patients. *Br J Cancer*. 1997;75:1049–1060.
16. De Bree R, Roos JC, Quak JJ, et al. Clinical screening of monoclonal antibodies 323/A3, cSF-25, and K928 for suitability of targeting tumors in the upper aerodigestive and respiratory tract. *Nucl Med Commun*. 1994;15:613–627.
17. Van Hal NLW, Van Dongen GAMS, Rood-Knippels EMC, et al. Monoclonal antibody U36, a suitable candidate for clinical immunotherapy of squamous cell carcinoma, recognizes a CD44 isoform. *Int J Cancer*. 1996;68:520–527.
18. Schrijvers AHGJ, Quak JJ, Uytendinck AM, et al. MAb U36: a novel monoclonal antibody successful in immunotargeting of squamous cell carcinoma of the head and neck. *Cancer Res*. 1993;53:4383–4390.
19. Heider K-H, Dämmrich J, Skroch-Angel P, et al. Differential expression of CD44 splice variants in intestinal- and diffuse-type human gastric carcinomas and normal gastric mucosa. *Cancer Res*. 1993;53:4197–4203.
20. Heider K-H, Sproll M, Susani S, et al. Characterization of a high-affinity monoclonal antibody specific for CD44v6 as candidate for immunotherapy of squamous cell carcinomas. *Cancer Immunol Immunother*. 1996;43:245–253.
21. Kaufmann M, Heider K-H, Sinn HP, et al. CD44 variant exon epitopes in primary breast cancer and length of survival. *Lancet*. 1995;345:615–619.
22. Mulder JW, Kruyt PM, Sewnath M, et al. Colorectal cancer prognosis and expression of exon-v6-containing CD44 proteins. *Lancet*. 1994;344:1470–1472.
23. Stauder R, Eistere W, Thaler J, Günthert U. CD44 variant isoforms in non-Hodgkin's lymphoma: a new independent prognostic factor. *Blood*. 1995;85:2885–2899.
24. Günthert U, Hofmann M, Rudy W, et al. A new variant of glycoprotein CD44 confers metastatic potential to rat carcinoma cells. *Cell*. 1991;65:13–24.
25. Heider K-H, Mulder J-WR, Ostermann E, et al. Splice variants of the cell surface glycoprotein CD44 associated with metastatic tumor cells are expressed in normal tissues of humans and cynomolgus monkeys. *Eur J Cancer*. 1995;31A:2385–2391.
26. Brakenhoff RH, Van Gog FB, Looney JE, et al. Construction and characterization of the chimeric monoclonal antibody E48 for therapy of head and neck cancer. *Cancer Immunol Immunother*. 1995;40:351–358.
27. Van Gog FB, Visser GWM, Stroomer JWG, et al. High dose rhenium-186 labeling of monoclonal antibodies for clinical application: pitfalls and solutions. *Cancer*. 1997;80:2360–2370.
28. Visser GWM, Gerretsen M, Herscheid JDM, Snow GB, Van Dongen GAMS. Labeling of monoclonal antibodies with ¹⁸⁶Re using the MAG3 chelate for radioimmunotherapy of cancer: a technical protocol. *J Nucl Med*. 1993;34:1953–1963.
29. Breitz HB, Fisher DR, Weiden PL, et al. Dosimetry of rhenium-186-labeled monoclonal antibodies: methods, prediction from technetium-99m-labeled antibodies and results of phase I trials. *J Nucl Med*. 1993;34:908–917.
30. Eary JF, Durack LD, Williams D, Vanderheyden J-L. Considerations for imaging Re-188 and Re-186 isotopes. *Clin Nucl Med*. 1990;15:911–916.
31. Buijs WCAM, Siegel JA, Boerman OC, Corstens FHM. Estimation of absolute organ activity using five different methods of background correction. *J Nucl Med*. 1998;39:2167–2172.
32. Shen S, DeNardo GL, Sgouros G, O'Donnell RT, DeNardo SJ. Practical determination of patient-specific marrow dose using radioactivity concentration in blood and body. *J Nucl Med*. 1999;40:2102–2106.
33. Sgouros G. Bone marrow dosimetry for radioimmunotherapy: theoretical considerations. *J Nucl Med*. 1993;34:689–694.
34. Maraveyas A, Myers M, Stafford N, et al. Radiolabeled antibody combined with external radiotherapy for the treatment of head and neck cancer: reconstruction of a theoretical phantom of the larynx for radiation dose calculation of local tissues. *Cancer Res*. 1995;55:1020–1027.
35. Gerretsen M, Visser GWM, Van Walsum M, et al. ¹⁸⁶Re-labeled monoclonal antibody E48 immunoglobulin G-mediated therapy of human head and neck squamous cell carcinoma xenografts. *Cancer Res*. 1993;53:3524–3529.
36. De Bree R, Kuik DJ, Quak JJ, et al. The impact of tumour volume and other characteristics on uptake of radiolabelled monoclonal antibodies in tumour tissue of head and neck cancer patients. *Eur J Nucl Med*. 1998;25:1562–1565.
37. Van Gog FB, Brakenhoff RH, Stigter-Van Walsum M, Van Dongen GAMS. Perspectives of combined radioimmunotherapy and anti-EGFR antibody therapy for the treatment of residual head and neck cancer. *Int J Cancer*. 1998;77:13–18.